A Comparison of Different Advective Solvers in the CHIMERE Air Quality Model

Pedro Molina[1], Luis Gavete[1], Marta García Vivanco[2], Inmaculada Palomino[2], M. Lucía Gavete[3], Francisco Ureña[4], and Juan José Benito[5]

[1] Universidad Politécnica de Madrid, Spain
[2] C.I.E.M.A.T. Madrid, Spain
[3] Universidad Rey Juan Carlos, Madrid, Spain
[4] Universidad Castilla-la Mancha, Ciudad Real, Spain
[5] U.N.E.D., Madrid, Spain
p.molina@upm.es, lu.gavete@upm.es, m.garcia@ciemat.es, inma.palomino@ciemat.es, lucia.gavete@urjc.es francisco.urena@uclm.es, jbenito@ind.uned.es

Abstract. Extensive research has been performed to solve the advection equation and different numerical methods have been proposed. Most of these methods, including semi-lagrangian methods, are not conservative. In this paper we compare in the CHIMERE eulerian chemistry transport model different conservative algorithms for solving the advection equation. The numerical results are compared with a set of observation sites in the area of Spain and some conclusions are obtained.

Keywords: advection equation, conservative scheme, Chimère.

1 Introduction

This paper is focused on air pollution modeling, a challenging scientific problem, specially in many industrialized countries where there is an increasing consciousness of the effect, on health and environment, of the emissions of pollutants into the urban atmospheres. The environmental benefits of reliable air quality forecasts are obvious: populations can be more efficiently protected by means of information or real-time emission abatement strategies.

Air pollution modeling is based on the assumption of no reciprocal effect of the chemical species on flow fields (wind velocity, turbulent diffusivity, temperature). After having pre-processed the flow fields by meteorological computations or parametrizations, the reaction-advection-diffusion PDE (Partial Differential Equation), that is, the mass continuity equation, is solved to estimate the concentrations of chemical species

$$\frac{\partial f}{\partial t} + \nabla\left(uf\right) = \nabla\left(k\nabla f\right) + P - L \tag{1}$$

.

In this equation, characteristic of the Eulerian approach, f is a vector containing the concentrations of all model species for every grid box, u is the three dimensional

B. Murgante et al. (Eds.): ICCSA 2011, Part IV, LNCS 6785, pp. 35–49, 2011.

wind vector, k the tensor of eddy diffusivity and P and L represent production and loss terms due to chemical reactions, emissions and deposition.

A class of conservative schemes for the advection equation has been so far proposed following the pioneering work of Godunov [1]. A Godunov type schemes computes the cell-integrated average values of a prognostic variable by using a conservative finite difference method of flux form, or a finite volume method as preferred by some researchers, and results in an exact conservation for the transported quantity. High order Godunov schemes can be devised by reconstructing high order interpolations within each mesh cell.

Rather than the piecewise constant interpolation in the original Godunov scheme, a linear interpolation function and a parabolic polynomial were used in the MUSCL[2,3] and the piecewise parabolic method (PPM) [4] schemes.

Other conservative schemes including a rational method can also be employed to solve the advection equation [5].

Basically, using a linear or higher order interpolation function for reconstruction tends to bring about oscillations to the numerical solutions. To get rid of this, slope modifications and the adjustments of the cell-interface values prove to be necessary. As a result, the piece-wisely constructed interpolation function is not usually continuous cross the cell interfaces.

Other studies have been carried out with the CHIMERE model but using only the PPM numerical solver[15].

Our main goal of this research is to compare three different algorithms for the transport module included in the European scale Eulerian chemistry transport model CHIMERE. The results of the different methods are compared with a set of observation sites in the area of the Iberian Peninsula in Spain.

Section 2 introduces the conservative methods that have been evaluated. In section 3 we introduce the European-scale chemistry-transport model (CHIMERE). The comparison of observed and modeled data is given in Section 4, and finally some conclusions are given in Section 5.

2 Modeling of Linear Advection 1D

For simplicity of presentation we start with the scalar advection problem in one space dimension. We note f as the concentration of one typical atmospheric pollutant. The advection in one space dimension of this pollutant, during the interval $[0,T]$ is given by the following linear hyperbolic equation, called also transport equation, to which we add an initial concentration; the overall Cauchy problem is consequently the following one.

Given a field of initial concentration $f(x,0) = f_0$, a velocity wind u and a time T > 0, we want to calculate $f(x,t)$ such that

$$\begin{cases} \dfrac{\partial f}{\partial x} + \dfrac{\partial (uf)}{\partial x} = 0 & \forall (x,t) \in \mathbb{R} \times [0,T] \\ f(x,0) = f_0(x) & \forall (x,t) \in \mathbb{R} \end{cases} \tag{2}$$

In the following sections it will be showed the three different finite volume methods to solving it.

The finite volume method is applied to the conservative form of the transport equation in one dimension in space. First we divide the spatial domain in cells called finite or controls volumes, this corresponds in one dimension to a partition of $[0,L] \subset \mathbb{R}$ by intervals, on the other hand one built discrete equations from the integral form of the equation.

Let be $\left(\left[x_{i-\frac{1}{2}}, x_{i+\frac{1}{2}} \right] \right)_{i \in \mathbb{Z}}$ a partition of $[0,L]$ and $([t^n, t^{n+1}])_{n \in \mathbb{N}}$ a regular partition of $[0,T]$. We define steps of time and space respectively written $\Delta t = t^{n+1} - t^n$ and $\Delta x_i = x_{i+\frac{1}{2}} - x_{i-\frac{1}{2}}$, the middle points $x_i = \frac{1}{2}\left(x_{i-\frac{1}{2}} + x_{i+\frac{1}{2}} \right)$ and the control volume $\Omega_i = \left[x_{i-\frac{1}{2}}, x_{i+\frac{1}{2}} \right]$.

By integrating (2) on $\Omega_i \times \left[t^n, t^{n+1} \right]$, we obtain the integral form of the conservation law

$$\rho_i^{n+1} = \rho_i^n - \frac{\Delta t}{\Delta x_i}\left(g^n_{i+\frac{1}{2}} - g^n_{i-\frac{1}{2}} \right) . \tag{3}$$

where we define the exact flux by

$$g^n_{i+\frac{1}{2}} = \frac{1}{\Delta x} \int_{t^n}^{t^{n+1}} (uf)\left(x_{i+\frac{1}{2}}, t \right) dt \tag{4}$$

and the average values of the exact solution, at the time t^n, on each cell by

$$\rho_i^n = \frac{1}{\Delta x} \int_{x_{i-\frac{1}{2}}}^{x_{i+\frac{1}{2}}} F(x, t^n) dx \ . \tag{5}$$

where F is the approximation of the function.

This equation is the finite volume formulation of the problem and belongs to the general framework of conservative schemes. In fact the conservative property means that the mass of specie A (with concentration f) is preserved (when time t move from t^n to t^{n+1}) only according to the boundaries conditions.

Three different approximations F_i are used in this paper corresponding to constant, linear and quadratic approximations of F_i over each one of the central cells.

By using time-splitting the method can be easily extended to solve advection equation in two and three dimensions. For example in two dimensions the time splitting is equivalent to do the transport of particles to the direction (Ox) and then according to the other direction (Oy).

2.1 The Upwind Method

The Godunov Method, or Upwind Method use a constant function a_i which is expressed in a generic mesh element with boundaries $x_{i-1/2}$, and $x_{i+1/2}$, and taking into account the velocity, u, the following constant approximation is used

$$\begin{aligned} F_i(x) &= a_i \quad \text{if } \mathrm{u} > 0 \\ F_i(x) &= a_{i-1} \quad \text{if } \mathrm{u} < 0 \end{aligned} \qquad \text{for } x \in \left[x_{i-1/2}, x_{i+1/2} \right] \tag{6}$$

where a_i is the value of the function in the initial moment where this value is known

$$F_i(x_{i-1/2}) = f^n_{i-1/2} = a_i \tag{7}$$

We can calculate the value of the flux for u>0, as follows

$$\begin{aligned} g^n_{i+\frac{1}{2}} &= \frac{1}{\Delta t} \int_{x_{i+1/2}-u^n_{i+1/2}\Delta t}^{x_{i+1/2}} F(x)dx = \frac{1}{\Delta t} \int_{x_{i+1/2}-u^n_{i+1/2}\Delta t}^{x_{i+1/2}} a_i dx = \frac{a_i}{\Delta t}(x)\Big|_{x_{i+1/2}-u^n_{i+1/2}\Delta t}^{x_{i+1/2}} = \\ &= \frac{a_i}{\Delta t}(x_{i+1/2} - (x_{i+1/2} - u^n_{i+1/2}\Delta t)) = \frac{a_i}{\Delta t} u^n_{i+1/2}\Delta t = u^n_{i+1/2} a_i \end{aligned} \tag{8}$$

where the superindex corresponds to the time step.

Then, we can completely explicit the flux function for the original Godunov method with respect to the value of the cell average integral ρ^n_i as follows

$$g_{i+\frac{1}{2}} = \begin{cases} \mathrm{u}^n_{i+\frac{1}{2}} \rho^n_i, & \text{if } \mathrm{u}^n_{i+\frac{1}{2}} > 0 \\ \mathrm{u}^n_{i+\frac{1}{2}} \rho^n_{i+\frac{1}{2}}, & \text{if } \mathrm{u}^n_{i+\frac{1}{2}} < 0 \end{cases} \tag{9}$$

2.2 VanLeer Method

The VanLeer method better known as MUSCLE or Monotocnic Upstream-Centered Scheme for Conservation Laws, using a minmod technique, use a linear function that is expressed in a generic mesh element with boundaries $x_{i-1/2}$, and $x_{i+1/2}$, and considering the velocity u < 0 as

$$F_i(x) = a_i + b_i(x - x_{i-1/2}) \quad \text{for } x \in \left[x_{i-1/2}, x_{i+1/2} \right] \tag{10}$$

where a_i, and b_i are the coefficients of the interpolation function.

a_i is calculated by the initial condition of each cell by

$$\begin{aligned} F_i(x_{i-1/2}) &= f^n_i \\ a_i &= f^n_i \end{aligned} \quad \text{if } u^n_{i+1/2} \geq 0$$

$$\begin{aligned} F_i(x_{i-1/2}) &= f^n_{i+1} \\ a_i &= f^n_{i+1} \end{aligned} \quad \text{if } u^n_{i+1/2} < 0 \tag{11}$$

To calculate the slope term of the interpolation function, b_i, we need to define a slope-limiter to assume a good relation between the interpolation function with the original function as the behavior of its monotonicity. A good choice of slope is given by minmod [4], as follows

$$\min \mathrm{mod} = b_i^n = \begin{cases} f_i - f_{i-1} & \text{if } (\delta f_{i-1/2} - \delta f_{i-3/2}) > 0 \\ f_{i-1} - f_{i-2} & \text{if } (\delta f_{i-1/2} - \delta f_{i-3/2}) > 0 \end{cases} . \tag{12}$$

were $\delta f_i = (f_i - f_{i-1})$.

Using (5) we can calculate the flux formulation, as follows

Monotonic case

$$g^n_{i+1/2} = \begin{cases} u^n_{i+1/2}\rho^n_i + (1 - CFL)u^n_{i+1/2}\Delta x_i b^n_i & \text{if } u^n_{i+1/2} \geq 0 \\ u^n_{i+1/2}\rho^n_{i+1} + (1 - CFL)u^n_{i+1/2}\Delta x_i b^n_i & \text{if } u^n_{i+1/2} < 0 \end{cases}$$

otherwise

$$g^n_{i+1/2} = \rho^n_i \quad . \tag{13}$$

where CFL is the Courant number, needed for the stability of the method, and it is calculated by

$$CFL = \left| \frac{u^n_i \Delta t}{\Delta x_i} \right| \tag{14}$$

We need three values $(\rho_{i-2}, \rho_{i-1}, \rho_i)$ to know the behavior of function's monotonicity.

2.3 Piecewise Parabolic Method (PPM)

The Piecewise Parabolic Method use a parabolic function, is expressed in a generic mesh element with boundaries $x_{i-1/2}$, and $x_{i+1/2}$, and considering the velocity u<0 as

$$F_i(x) = a_i + b_i \overline{X}_i + c_i \overline{X}_i (1 - \overline{X}_i) \quad \text{for } x \in \left[x_{i-1/2}, x_{i+1/2} \right] . \tag{15}$$

where

$$\overline{X}_i = \frac{1}{\Delta x_i}(x - x_{i-1/2}) .$$

a_i, bi and c_i are the coefficients of the interpolation function which are obtained by using the constraint conditions, where the constraint conditions are given in each cell by

$$
\begin{aligned}
&F_i(x_{i-1/2}) = f^n_{i-1/2} \\
&F_i(x_{i+1/2}) = f^n_{i+1/2} \\
&\frac{1}{\Delta x_i}\int_{x_{i-1/2}}^{x_{i+1/2}} F_i(x)dx = \rho^n_i
\end{aligned}
\quad . \tag{16}
$$

where $\Delta x_i = x_{i+1/2} - x_{i-1/2}$.

Then the coefficients a_i, b_i and c_i are given by

$$
\begin{aligned}
&a_i = F_i(x_{i-1/2}) \\
&b_i = F_i(x_{i+1/2}) - F_i(x_{i-1/2}) \\
&c_i = 6\left(f_i - \frac{1}{2}(F_i(x_{i-1/2}) + F_i(x_{i+1/2}))\right)
\end{aligned}
\quad . \tag{17}
$$

It is well-known that any high order interpolation tends to create spurious oscillations in numerical solutions. As a remedy for this, slope modifications were introduced in the PPM schemes. In this paper, we adopted the method of Colella and Woodward [4] for computing the interface values as,

$$
f^n_{i+1/2} = \frac{1}{2}(\rho^n_i + \rho^n_{i+1}) - \frac{1}{6}(\overline{\delta} f^n_i - \overline{\delta} f^n_{i-1}) \quad . \tag{18}
$$

with $\overline{\delta} f^n_i$ being the average slope in cell $\left[x_{i-1/2}, x_{i+1/2}\right]$ as follows

$$
\overline{\delta} f_i = \begin{cases} 2\cdot\min(\delta f_i, \alpha_1(\rho_{i+1} - \rho_i), \alpha_2(\rho_i + \rho_{i-1})), & \text{if } (\rho_{i+1} - \rho_i) > 0 \\ 2\cdot\max(\delta f_i, \alpha_1(\rho_{i+1} - \rho_i), \alpha_2(\rho_i + \rho_{i-1})), & \text{if } (\rho_{i+1} - \rho_i) < 0 \end{cases} \quad . \tag{19}
$$

were $\delta f_i = (\rho_{i+1} - \rho_{i-1})/4$. The positives α_1 and α_2 are parameters that control the average slope and affect the dispersion errors of the numerical solutions. For the piecewise parabolic method used in Chimère $\alpha_1 = \alpha_2 = 1$.

To insurance good properties for the reconstruction we must to insure the parabolic monotonicity built on each cell. Then a second corrector algorithm is used to assume the monotonicity.

The flux calculation is given by

$$
g^n_{i+1/2} = \begin{cases} u^n_{i+1/2}\left(F_i(x_{i+1/2}) - \frac{1}{2}CFL\left(\Delta a_i - \left(1 - \frac{2}{3}\frac{u^n_{i+1/2}\Delta t}{\Delta x_i}\right)c_i\right)\right), & if\ u^n_{i+1/2} \geq 0 \\ u^n_{i+1/2}\left(F_{i+1}(x_{i+1/2}) - \frac{1}{2}CFL\left(\Delta a_{i+1} + \left(1 + \frac{2}{3}\frac{u^n_{i+1/2}\Delta t}{\Delta x_{i+1}}\right)c_{i+1}\right)\right), & if\ u^n_{i+1/2} < 0 \end{cases} . \tag{20}
$$

where $\mathrm{CFL} = \left| \frac{u^n_{i+1/2}\Delta t}{\Delta x_i} \right|$

3 Chemical Model Description

The numerical method for the temporal solution of the stiff system of partial differential equations which defines the chemical reactions in the atmosphere is adapted from the second-order TWO-STEP algorithm originally proposed by [6] for gas phase chemistry only. It is based on the application of a Gauss-Seidel iteration scheme to the 2-step implicit backward differentiation (BDF2) formula

$$f^{n+1} = \frac{4}{3} f^{n} - \frac{1}{3} f^{n-1} + \frac{2}{3} \Delta t R(f^{n+1}) \ . \tag{21}$$

with f^n being the vector of chemical concentrations at time t^n, Δt the time step leading from time t^n to t^{n+1} and $R_{(f)} = P_{(f)} - L_{(f)}$ the temporal evolution of the concentrations due to chemical production and emissions (P) and chemical loss and deposition (L). Note that L is a diagonal matrix here. After rearranging and introducing the production and loss terms this equation reads

$$f^{n+1} = \left(I + \frac{2}{3} \Delta t L(f^{n+1}) \right)^{-1} \left(\frac{4}{3} f^{n} - \frac{1}{3} f^{n-1} + \frac{2}{3} \Delta t P(f^{n+1}) \right) . \tag{22}$$

The implicit nonlinear system obtained in this scheme can be solved pertinently with a Gauss-Seidel method [6]. The obtained values of L and P due to the chemical reactions are added in equation (1). A more complete description and evaluation of the CHIMERE model for seasonal simulations and real time forecasts without the use of super-computers, can be found in [7].

4 Numerical Results

Simulations were carried out using the regional V2008 version of the CHIMERE model for 2007. This version calculates the concentration of 44 gaseous species and both inorganic and organic aerosols of primary and secondary origin, including primary particulate matter, mineral dust, sulfate, nitrate, ammonium, secondary organic species and water. The effect of the different numerical resolution scheme on model estimates was analyzed for a domain centred on the Iberian Peninsula in Spain (SP in Figure 2). This simulation scheme was to that used in [9]; A finer domain at a horizontal resolution of 0.2 degree and , covering the Iberian Peninsula was nested to a coarser European scale domain (EUR in Figure 2), ranging from 10.5W to 22.5E and from 35N to 57.5 N and a 0.5 degree horizontal resolution. A one-way nesting procedure was used: coarse-grid simulations forced the fine-grid ones at the boundaries without feedback.

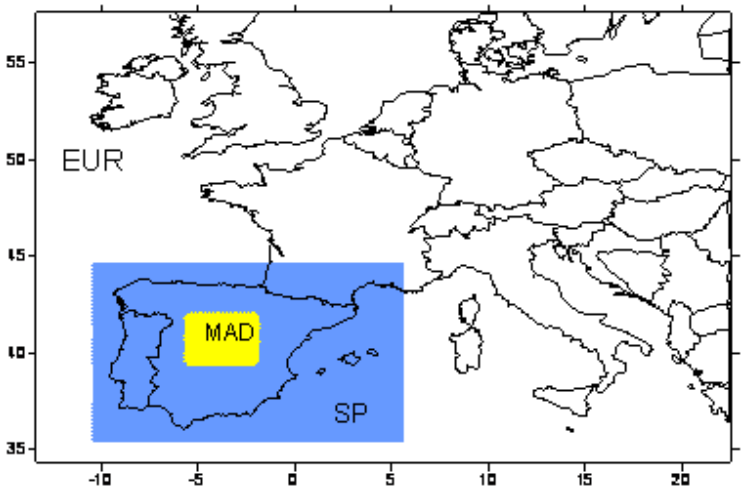

Fig. 1. Location of the two domains simulated with the CHIMERE model

Boundary conditions for the coarsest domain were provided from monthly 2006 climatology from LMDz-INCA model [10] for gases concentrations and from monthly 2004 GOCART model [11] for particulate species.

Accurate emissions data in each time step are not available, then emissions for all the simulations were derived from the annual totals of the EMEP database for 2007 [12]. Original EMEP emissions were spatially disaggregated taking into account land use information (Global Land Cover Facility, GLCF, http://change.gsfc.nasa.gov/create.html) in order to get higher resolution emission data. For each SNAP activity sector, the total NMVOC emission was split into emissions of 227 real individual NMVOC, according to the AEAT speciation [13]. These species were then aggregated into the CHIMERE model ones.

The MM5 model was used to obtain the meteorological input fields. The simulations were carried out also for two domains, with respective horizontal resolutions of 36 Km and 19 Km. Both MM5 simulations were forced by the National Centres for Environmental Prediction model (GFS) analyses.

The CHIMERE model was used with a time step of 3.3 minutes for the three methods.

The quality of model predictions obtained with the three algorithms for the transport module was analyzed by comparing model results to observations at the monitoring sites. Figure 3 shows the location of the NO_2, NO_x SO_2, O_3, and PM_{10} monitoring stations located inside the domain. Figures 5, 6, 7 and 8 present NO_x, O_3, SO_2, and PM_{10} time series showing the concentration obtained with the three methods and the values registered at one of the monitoring sites (01016001 station, Figure 4) for the period between June, 30th and August, 3th in 2007, as an example of the model performance.

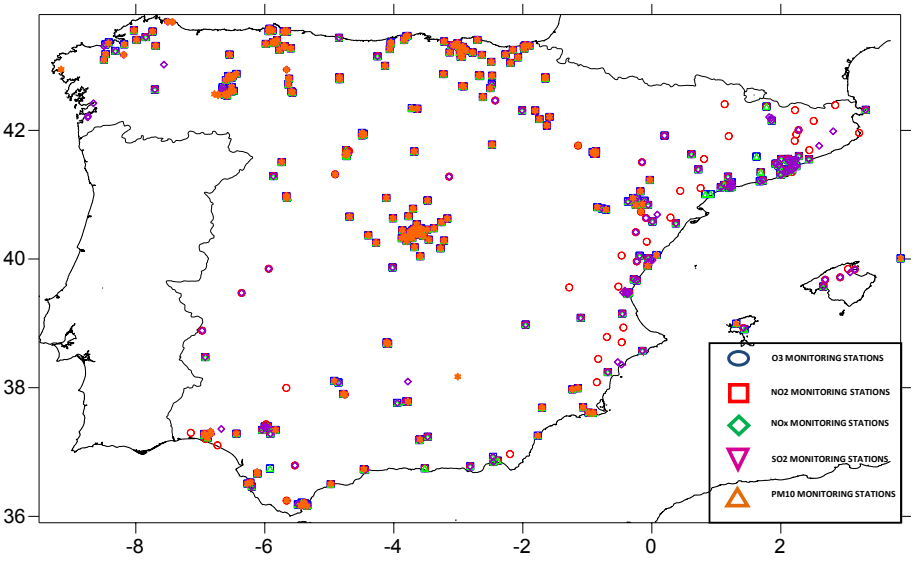

Fig. 2. Location of the monitoring sites recording NO_2, NO_x, SO_2,PM_{10} and O_3 in Spain in 2007

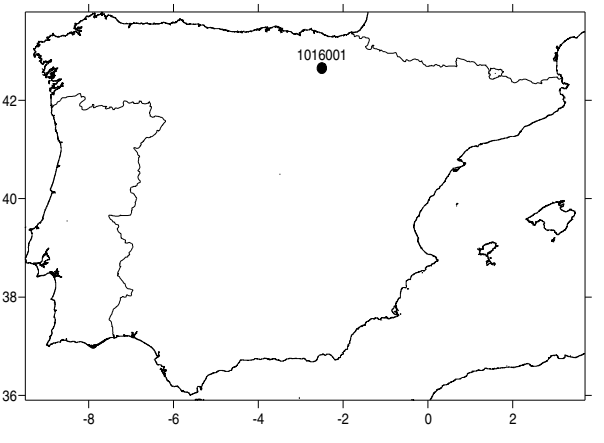

Fig. 3. Location of the 01016001 monitoring station

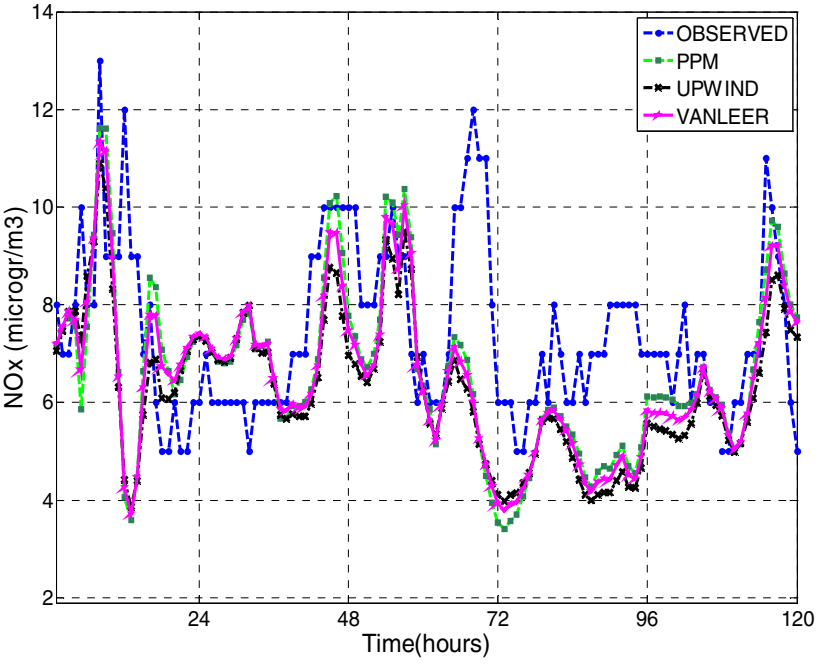

Fig. 4. Observed and simulated NO_x concentration at 01016001 station

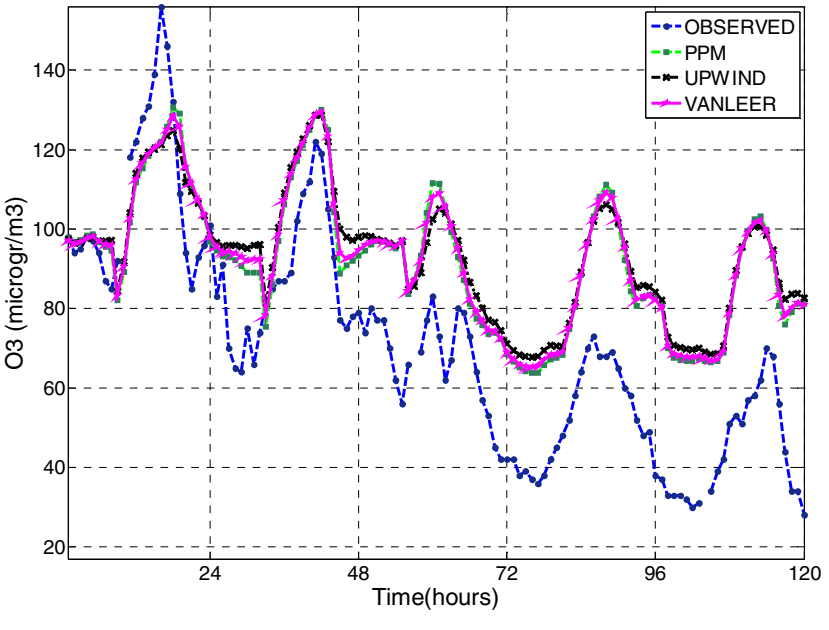

Fig. 5. Observed and simulated O_3 concentration at 01016001 station

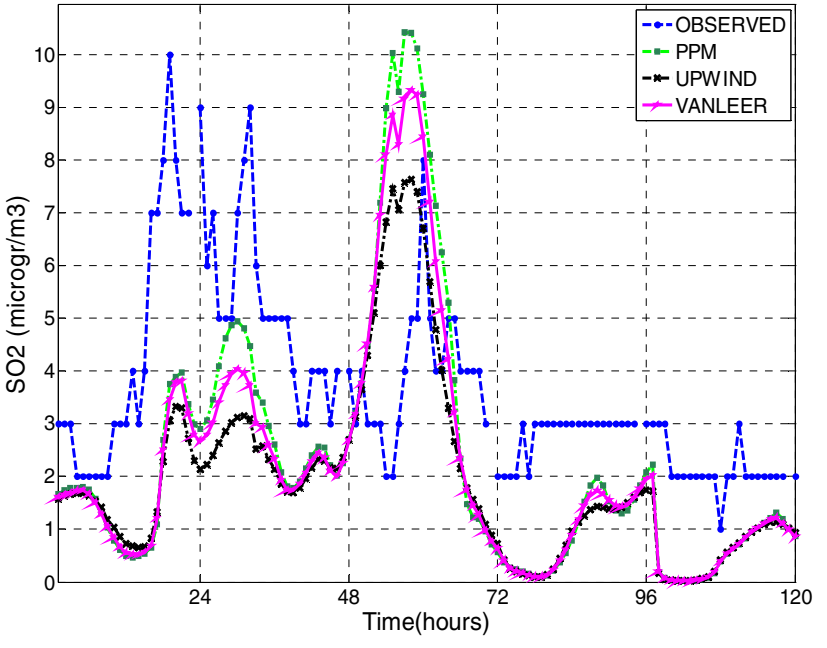

Fig. 6. Observed and simulated SO_2 concentration at 01016001 station

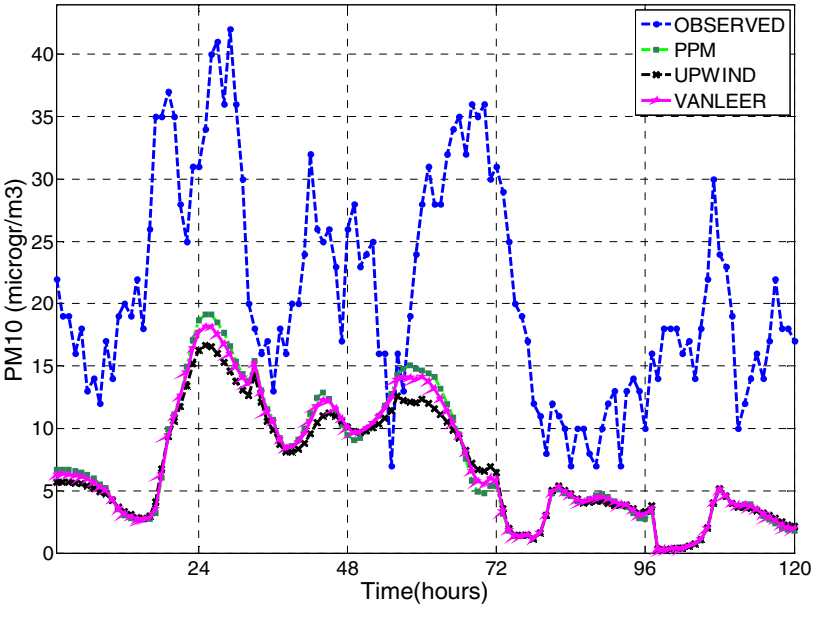

Fig. 7. Observed and simulated PM_{10} concentration at 01016001 station

Table 1. Definition of the metrics used in the evaluation of the CHIMERE model performance

Mean bias	$B_{MB} = \frac{1}{N}\sum(M_i - O_i) = \overline{M} - \overline{O}$
Mean normalized bias	$B_{MNB} = \frac{1}{N}\Sigma\left(\frac{M_i - O_i}{O_i}\right) = \left(\frac{1}{N}\Sigma\frac{M_i}{O_i} - 1\right)$
Mean normalized absolute error	$E_{MNAE} = \frac{1}{N}\Sigma\left(\frac{\lvert M_i - O_i\rvert}{O_i}\right)$
Root mean square error	$E_{RMSE} = \left[\frac{1}{N}\sum(M_i - O_i)^2\right]^{\frac{1}{2}}$
Root mean normalized square error	$E_{RMNSE} = \left[\frac{1}{N}\Sigma\left(\frac{M_i - O_i}{O_i}\right)^2\right]^{\frac{1}{2}}$

N: pairs of modeled and observed concentrations *Mi* and *Oi.* The index *i* is over time series and over all the locations in the domain. * $\overline{M} = \frac{1}{N}\sum M_i \overline{O} = \frac{1}{N}\sum O_i$.

Table 2. Mean Concentration for observed and simulated pollutant with the three different conservative methods

	NO_2				SO_2				O_3			
Station	Observed	Upwind	Vanleer	PPM	Observed	Upwind	Vanleer	PPM	Observed	Upwind	Vanleer	PPM
1016001	4.7866	6.2246	6.3935	6.489	3.1098	1.1537	1.2398	1.31	73.5554	88.5497	87.6326	87.0642
1055001	9.4117	6.5169	6.6793	6.774	3.6507	1.371	1.4688	1.5237	69.6142	84.6495	83.8801	83.3886
6016999	3.3103	6.6538	6.7025	6.737	1.4735	0.5893	0.5912	0.6007	74.0728	88.1028	87.8342	87.7665
12032001	10.9689	11.1228	11.3921	11.65	3.8059	2.4019	2.4747	2.5252	31.9679	99.0982	98.4951	97.8441
12099001	8.7443	8.0439	8.249	8.381	4.9698	2.5303	2.899	3.1748	67.9787	93.1618	92.5146	91.9271
12127002	6.8648	5.5356	5.6136	5.673	91.2196	98.3157	98.1126	97.9295	7.8644	3.6566	3.9096	4.0000
15070006	2.5303	5.3069	5.3401	5.368	3.1528	5.1946	4.877	4.5892	36.1126	68.8811	67.7442	67.3601
27033001	2.7271	5.0501	5.0266	5.007	13.0682	17.282	16.7511	16.3985	55.675	69.4079	68.559	68.3416
27058999	3.2231	5.3446	5.3904	5.402	4.0529	4.5851	4.5566	4.4867	56.9156	72.872	72.0308	71.692
27065004	3.1986	5.3884	5.3868	5.383	11.3763	15.5587	15.6326	15.6811	44.8347	70.2854	69.3949	69.0793
31107001	3.01	6.0139	6.198	6.291	3.9642	0.6581	0.7146	0.7553	85.9682	88.8763	87.7539	87.1223
31232002	8.4504	6.2111	6.4245	6.555	3.2836	0.5689	0.6258	0.6717	69.4824	87.1073	86.0155	85.3741
33031029	20.3268	10.3993	10.5258	10.65	10.4492	8.2066	8.347	8.4698	32.6792	73.6432	72.5261	71.7362
43005002	5.4196	10.0196	10.0342	10.06	8.3955	2.4806	2.3846	2.3124	67.7855	92.1313	91.7707	91.4043
44051002	1.2951	6.5892	6.6021	6.635	1.9179	7.482	7.4566	7.5252	83.2927	92.8247	92.2461	91.9131
44118001	4.7056	6.339	6.3015	6.292	8.9103	6.4856	6.6358	6.721	79.383	90.3541	89.9555	89.701

In order to evaluate the performance of the CHIMERE model estimates using the three different models some statistics were calculated. Table 2 presents the metrics used and their definition. Parameters such as mean bias (BMB), mean normalized bias (BMNB), mean normalized absolute error (EMNAE), root mean square error (ERMSE) and root mean normalized square error (ERMNSE) were estimated for NO_2, NO_x, SO_2, O_3 and PM_{10}. Regarding ozone, only statistics for moderate-to-high

ozone concentration cases (more important for human health protection) were considered by selecting predicted-observed value pairs when hourly observations were equal to or greater than the cutoff of 80 μgm^{-3}. For NO_2, NO_x, SO_2 and PM_{10} a cutoff value of 10μgm^{-3} was used. It was taken into account 73, 76, 72, 86 and 54 air quality sites to estimate the statistics of O_3, NO_x, SO_2 and PM_{10} respectively.

In table 3 we show the mean observed and simulated concentration of some pollutants at 16 monitoring stations. Statistical results for all the pollutants are presented in Table 4. Mean normalized bias and mean normalized absolute error for ozone present values inside the range proposed by Tesche et al.[14] to decide on the suitability of a model.

Table 3. Statistics for all the pollutants evaluation for July 2007

O_3	**BMB**	**BMNB**	**EMNAE**	**ERMSE**	**ERMNSE**
Uwind	-1.7035	-0.0052	12.90%	16.9665	16.54%
Van Leer	-1.8389	-0.0069	12.99%	17.0798	16.66%
PPM	-2.0593	-0.0093	13.06%	17.187	16.74%
NO_2					
Uwind	-10.0749	-0.426	61.10%	17.5791	74.83%
Van Leer	-10.0465	-0.4237	61.35%	17.6013	75.44%
PPM	-10.0409	-0.4228	61.53%	17.596	75.79%
NO_x					
Uwind	-14.7716	-0.4768	66.81%	27.7608	81.24%
Van Leer	-14.739	-0.4747	67.04%	27.8095	82.14%
PPM	-14.7318	-0.4741	67.19%	27.828	82.66%
SO_2					
Uwind	-27.5862	-0.6279	76.51%	57.4427	85.92%
Van Leer	-27.5404	-0.6243	77.07%	57.5217	87.10%
PPM	-27.5213	-0.6225	77.68%	57.6022	88.33%
PM_{10}					
Uwind	-21.1558	-0.7469	74.88%	26.9477	76.88%
Van Leer	-21.1623	-0.748	75.03%	26.9582	77.11%
PPM	-21.1913	-0.7498	75.24%	26.9839	77.37%

5 Conclusions

In this paper we have compared the concentration of some pollutants predicted by the CHIMERE Eulerian chemistry transport model using three different conservative methods to solve the advection equation.

The advantage of these methods is that the cell-integrated average is predicted via a flux formulation, thus the mass is exactly conserved. The simulated concentrations for all the pollutants have been compared with a set of observation registered at some monitoring sites in Spain. There are some EPA guidelines to evaluate the accuracy of ozone model predictions (Tesche et al.[14]). The mean normalized absolute error, included in these guidelines, present, for ozone, values inside the ranges proposed inside the suggested EPA range (30-35%), (see Table 4), in order to consider an

acceptable model performance. For the other pollutants, errors present higher values, as it commonly found when evaluating air quality model performance with EMEP database. The disagreement between model and observations for these pollutants is more related to accuracy of the input information, such as emissions, meteorology or land use data. For the time increment used the three advection solvers give similar results, using the 19 km resolution.

If the three advection solvers give similar results, it can be due to the very smooth functions calculated in the emission temporal disaggregation. As conclusion it appears that the type of algorithm used for the advection problem is not so determninant. As it is important to decrease the execution time then, it is sufficient to use the upwind method which is the faster one.

Acknowledgements

This study was supported by Ministerio de Ciencia y Tecnología of Spain under the project CGL2008-1757/CLI.

References

1. Godunov, S.K.: A difference scheme for numerical computation of discontinuous solutions of hydrodynamics equations. Math. Sbornik 47, 271–306 (1959) (in Russian)
2. van Leer, B.: Toward the ultimate conservative difference scheme. Part IV: A new approach to numerical convection. J. Comput. Phys. 23, 276–299 (1997)
3. van Leer, B.: Toward the ultimate conservative difference scheme. Part V: A second order sequel to Godunov's method. J. Comput. Phys. 23, 276–299 (1997)
4. Collela, P., Woodward, P.R.: The piecewise parabolic method (PPM) for gas-dynamical simulations. J. Comput. Phys. 54, 174–201 (1984)
5. Gavete, L., García Vivanco, M., Molina, P., Gavete, M.L., Ureña, F., Benito, J.J.: Implementation in Chimère of a conservative solver for the advection equation. In: Proceedings of the 10th International Conference on Mathematical Methods in Science and Engineering, vol. IV, pp. 1094–1105. CMMSE, Almería (2010), ISBN 13: 978-84-613-5510-5
6. Le Veque, R.J.: Numerical Methods for Conservation Laws. Birkuser Verlag (1990)
7. Verwer, J.G.: A Gauss-Seidel iteration for stiff ODEs from chemical kinetics. SIAM J. Scientific Computing 15, 1243–1250 (1994)
8. Schmidt, H., Derognat, C., Vautard, R., Beekmann, M.: A comparision of simulated and observed ozone mixing ratios for the summer of 1998 in Western Europe. Atmospheric Environment 35, 6277–6297 (2001)
9. Vivanco, M.G., Palomino, I., Vautard, R., Bessagnet, B., Martín, F., Menut, L., Jiménez, S.: Multi-year assessment of photochemical air quality simulation over SPAIN. Environmental Modelling & Software 24, 63–73 (2009)
10. Hauglustaine, D.A., Hourdin, F., Jourdain, L., Filiberti, M.A., Walters, S., Lamarque, J.F., Holland, E.A.: Interactive chemistry in the Laboratoire de Meteorologie Dynamique general circulation model: Description and background tropospheric chemistry evaluation. J. Geophys. Res. 109 (2004), doi:10.1029/2003JD003957

11. Chin, M., Ginoux, P., Kinne, S., Holben, B.N., Duncan, B.N., Martin, R.V., Logan, J.A., Higurashi, A., Nakajima, T.: Tropospheric aerosol optical thickness fromt he GOCART model and comparisons with satellite and sunphotometer measurements. J. Atmos. Sci. 59, 461–483 (2002)
12. Vestreng, V., Breivik, K., Adams, M., Wagener, A., Goodwin, J., Rozovskkaya, O., Pacyna, J.M.: Inventory Review 2005, Emission Data reported to LRTAP Convention and NEC Directive, Initial review of HMs and POPs. Technical report MSC-W 1/(2005), ISSN 0804-2446
13. Passant, N.R.: Speciation of UK Emissions of Non-methane Volatile Organic Compounds. AEAT/ENV/R/0545 (1) (2000)
14. Tesche, T.W., Georgopoulos, P., Seinfeld, J.H., Cass, G., Lurmann, F.W., Roth, P.M.: Improvement of Procedures for Evaluating Photochemical Models. Draft Final Report Prepared for California Air Resources Board. Radian, Sacramento (1990)
15. Vivanco, M.G., Correa, M., Azula, O., Palomino, I., Martín, F.: Influence of Model Resolution on Ozone Predictions over Madrid Area (Spain). In: Gervasi, O., Murgante, B., Laganà, A., Taniar, D., Mun, Y., Gavrilova, M.L. (eds.) ICCSA 2008, Part I. LNCS, vol. 5072, pp. 165–178. Springer, Heidelberg (2008)